International Journal of Automotive Technology, Vol. 12, No. 3, pp. 391−399 (2011)
DOI 10.1007/s12239−011−0046−4

1229−9138/2011/058−10

DESIGN AND EVALUATION OF SIDESLIP ANGLE OBSERVER FOR VEHICLE STABILITY CONTROL

D. W. PI[1)*], N. CHEN[2)], J. X. WANG[2)] and B. J. ZHANG[3)]

[1)]School of Mechanical Engineering, Nanjing University of Science and Technology, Nanjing 210094, China
[2)]School of Mechanical Engineering, Southeast University, Nanjing 211189, China
[3)]Commercial Vehicle R&D Center, SAIC Motor, 100 Hongshan Road, Jiangsu, Nanjing 210028, China

(Received 6 April 2009; Revised 19 October 2010)

ABSTRACT−This paper presents a method for estimating the vehicle side slip angle, which is considered as a significant signal in determining the vehicle stability region in vehicle stability control systems. The proposed method combines the model-based method and kinematics-based method. Side forces of the front and rear axles are provided as a weighted sum of directly calculated values from a lateral acceleration sensor and a yaw rate sensor and from a tire model according to the nonlinear factor, which is defined to identify the degree of nonlinearity of the vehicle state. Then, the side forces are fed to the extended Kalman filter, which is designed based on the single-track vehicle model associated with a tire model. The cornering stiffness identifier is introduced to compensate for tire force nonlinearities. A fuzzy-logic procedure is implemented to determine the nonlinear factor from the input variables: yaw rate deviation from the reference value and lateral acceleration. The proposed observer is compared with a model-based method and kinematics-based method. An 8 DOF vehicle model and Dugoff tire model are employed to simulate the vehicle state in MATLAB/SIMULINK. The simulation results shows that the proposed method is more accurate than the model-based method and kinematics-based method when the vehicle is subjected to severe maneuvers under different road conditions.

KEY WORDS : Side slip angle, Estimation method, Extended Kalman filter, Nonlinear factor, VSC (Vehicle Stability Control)

1. INTRODUCTION

Recently, vehicle stability control systems have been studied actively for the improvement of vehicle stability and handling predictability. A vehicle stability control (VSC) system can utilize differential braking to generate the stabilizing yaw moment to prevent vehicle spin and drift out. These systems use the sideslip angle as a critical component of the control logic (Van Zanten *et al*., 1996; Mammar and Koenig, 2002; Masato *et al*., 2001; Jo *et al*., 2008). Sideslip angle can be measured accurately using a two antenna global positioning system (GPS) without knowledge of the vehicle model (Bevly *et al*., 2006; Daily and Bevly, 2004). It can also be directly measured by sensors based on optical methods or supersonic waves. However, these direct measurement methods represent a disproportionate cost in the case of production cars. Hence, many kinds of observers are proposed to solve this problem.

The observers proposed can be divided into three groups: kinematics-based methods (Chen and Hsieh, 2008; Van Zanten, 2000; Park *et al*., 2001), model-based methods (Hac and Simpson, 2000; Keinke and Daiâ, 1997; Hiraoka *et al*., 2004; Stephant *et al*., 2004) and combined methods (Cheli *et al*., 2007; Piyabongkarn *et al*., 2006; Nishio *et al*., 2001; Fukada, 1999). The kinematics-based method integrates the derivative of side-slip angle calculated from sensor signals including yaw rate, lateral acceleration and vehicle speed. It can achieve good robustness against tire properties, road friction and vehicle parameters such as vehicle mass and moment of inertia. However, the integration can cause a drift when sensing errors or when road slant angles exist. The model-based method is proposed to solve the convergence problem caused by road bank angle and sensor errors. However, the model-based method strongly depends on the accuracy of the vehicle parameters. Stephant *et al*. (2004) present a typical structure of this method based on on-board vehicle models. The author stated four observers, including a linear observer based on a linear vehicle model, an extended Luenberger observer, an extended Kalman filter and a sliding-mode observer based on an extended nonlinear vehicle model. Within the linear regions, all proposed observers are satisfactory and give approximately the same results. However, the accuracy in the nonlinear regions deteriorates due to the linearity assumption. The combined method combines the advantages of the previous two methods. The algorithm proposed in Piyabongkarn *et al*. (2006) selects an adaptive filter parameter according to the frequency of lateral acceleration. The value from the model-

**Corresponding author.* e-mail: pidawei@gmail.com

based method plays an important role at low frequencies while the weight of the kinematics-based method is relatively large at higher frequency. However, this method is an open loop observer, and large estimation errors might result from not only signal offsets and noises but also large roll and pitch motions. Furthermore, it can be difficult to find the best balance between the model-based estimation and kinematics-based estimation. The determination of the adaptive filter parameter can greatly affect the performance of estimation method. To minimize these effects, the error signals, which is the differences between the measured signals and predicted values by the model, can be introduced to form a closed loop observer.

In this paper, a closed loop estimation strategy that combines the model-based method and kinematics-based method is presented. The schematic representation of the proposed slip angle estimation methodology is shown in Figure 1, where the input signals are acquired through the on-board sensors. The block provides the side force calculated from sensor via the kinematics-based method, and simultaneously, the tire model generates the side force following the model-based method. These generated side forces are then weighted and summed according to the degree of vehicle nonlinear state, which is defined through a fuzzy-logic procedure considering the yaw rate deviation and lateral acceleration. An extended Kalman filter based on the single-track vehicle model is employed to compute the estimation of the side slip angle. In addition, an identifier for the cornering stiffness is adopted to take into account the nonlinearity of the tire properties. To evaluate the performance of the proposed estimation methodology, the simulation is conducted under severe driving scenarios and different road friction conditions in Matlab/Simulink, where a nonlinear vehicle model is adopted in place of the real vehicle. Simulation results of the proposed estimation strategy are compared with the model-based method and kinematics-based method.

The second section of this paper describes a nonlinear vehicle model and tire model constructed as a simulation plant. Next, the model-based and kinematics-based method is presented in section 3. The proposed estimator is presented in section 4. The simulation results and comparison of different observers are given in section 5. Finally, conclusions are presented in section 6.

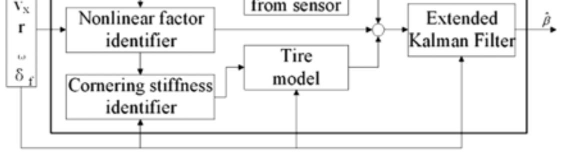

Figure 1. Scheme of the proposed estimation method.

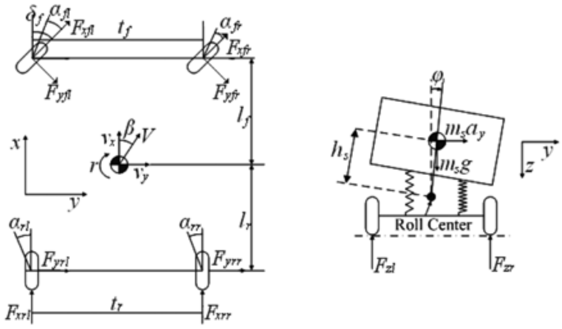

Figure 2. Nonlinear vehicle model.

2. VEHICLE MODELING FOR SIMULATION

2.1. Vehicle Model

A nonlinear vehicle handling model is constructed to evaluate the proposed estimation method. This model consists of 8DOF, which include lateral and longitudinal velocity (v_x, v_y), yaw rate (r) and body roll rate (p) as well as the wheel rotational speed (ω_{fl}, ω_{fr}, ω_{rl}, ω_{rr}). The vehicle body-fixed coordinate system is used to set up the model. The equations of motion derived from Figure 2 are as follows:

Longitudinal motion:

$$m(\dot{v}_x - rv_y) + m_s h_s r\dot{\varphi} = (F_{xfl}+F_{xfr})\cos\delta_f - (F_{yfl}+F_{yfr})\sin\delta_f + F_{xrl} + F_{xrr} \tag{1}$$

Lateral motion:

$$m(\dot{v}_y + rv_x) - m_s h_s r\ddot{\varphi} = (F_{xfl}+F_{xfr})\sin\delta_f + (F_{yfl}+F_{yfr})\cos\delta_f + F_{xrl} + F_{xrr} \tag{2}$$

Yaw motion:

$$\begin{aligned} I_{zz}\dot{r} &= l_f((F_{xfl}+F_{xfr})\sin\delta_f + (F_{yfl}+F_{yfr})\cos\delta_f) \\ &-\frac{t_f}{2}((F_{xfr}-F_{xfl})\cos\delta_f + (F_{yfl}-F_{yfr})\sin\delta_f) \\ &+\frac{t_r}{2}(F_{xrl}-F_{xrr}) - l_r(F_{yrl}+F_{yrr}) + I_{xz}\ddot{\varphi} \end{aligned} \tag{3}$$

Roll motion:

$$I_{xx}\ddot{\varphi} = [m_s g h_s - (K_{\varphi f}+K_{\varphi r})]\varphi - (C_{\varphi f}+C_{\varphi r})\dot{\varphi} + I_{xz}\dot{r} - m_s h_s(\dot{v}_y + v_x r) \tag{4}$$

$$\dot{\varphi} = p \tag{5}$$

Wheel rotational motion:

$$I_\omega \omega_i = -R_\omega F_{xi} + T_i \quad i = (fl, fr, rl, rr) \tag{6}$$

where T_i, with i=fl,fr,rl,rr, is the sum of the driving torque and the brake torque applied to the ith wheel.

The terms F_{xi} and F_{yi} are the respective longitudinal force and lateral force in the vehicle body-fixed coordinate system from the corresponding tire. Because the tire force is generated in a wheel-fixed coordinate system, the lateral and longitudinal tire force must be multiplied by the corresponding sine and cosine of the steer angle for each wheel to convert it to the vehicle body-fixed coordinate. φ is the vehicle body roll angle.

2.2. Tire Model

To simulate the limit handling situations, the Dugoff model (Dugoff *et al.*, 1970) is introduced to calculate the lateral and longitudinal forces generated by tires. The longitudinal and lateral forces are determined by the following equations:

$$\lambda_i = \frac{\mu F_{zi}(1+\sigma_{xi})(1-\varepsilon_v v_x(\sigma_{xi}^2+(\tan(\alpha_i))^2)^{1/2})}{2[(C_\sigma \sigma_{xi})^2+(C_\alpha \tan(\alpha_i))^2]^{1/2}} \tag{7}$$

$$f_i(\lambda_i) = \begin{cases} (2-\lambda_i)\lambda_i & (\lambda_i<1) \\ 1 & (\lambda_i \geq 1) \end{cases} \tag{8}$$

$$F_{xi} = C_\sigma \frac{\sigma_{xi}}{1+\sigma_{xi}} f(\lambda_i) \tag{9}$$

$$F_{yi} = C_\alpha \frac{\tan(\alpha_i)}{1+\sigma_{xi}} f(\lambda_i) \tag{10}$$

where i=fl,fr,rl,rr, μ is the road friction coefficient and ε_v is the velocity effect factor.

This model includes a quasi-static lateral and longitudinal load transfer. Thus, the normal load equation for each wheel can be expressed as:

$$F_{zfl} = \frac{mgl_r}{2l} + \frac{1}{t_f}(-K_{\varphi f}\varphi - C_{\varphi f}\dot{\varphi}) - \frac{ma_x h_{cg}}{2l} + \frac{a_y}{t_f}\left(\frac{m_s l_{rs} h_f}{l} + m_{uf} h_{uf}\right) \tag{11}$$

$$F_{zfl} = \frac{mgl_r}{2l} - \frac{1}{t_f}(-K_{\varphi f}\varphi - C_{\varphi f}\dot{\varphi}) - \frac{ma_x h_{cg}}{2l} - \frac{a_y}{t_f}\left(\frac{m_s l_{rs} h_f}{l} + m_{uf} h_{uf}\right) \tag{12}$$

$$F_{zrl} = \frac{mgl_f}{2l} + \frac{1}{t_r}(-K_{\varphi r}\varphi - C_{\varphi r}\dot{\varphi}) + \frac{ma_x h_{cg}}{2l} + \frac{a_y}{t_f}\left(\frac{m_s l_{fs} h_r}{l} + m_{ur} h_{ur}\right) \tag{13}$$

$$F_{zrr} = \frac{mgl_f}{2l} - \frac{1}{t_r}(-K_{\varphi r}\varphi - C_{\varphi r}\dot{\varphi}) + \frac{ma_x h_{cg}}{2l} - \frac{a_y}{t_f}\left(\frac{m_s l_{fs} h_r}{l} + m_{ur} h_{ur}\right) \tag{14}$$

The tire sideslip angle α_i(i=fl,fr,rl,rr) for each wheel can be calculated as:

$$\alpha_{fl} = \arctan\left(\frac{v_y + l_f r}{v_x - (t_f/2)r}\right) - \delta_f \tag{15}$$

$$\alpha_{fr} = \arctan\left(\frac{v_y + l_f r}{v_x + (t_f/2)r}\right) - \delta_f \tag{16}$$

$$\alpha_{rl} = \arctan\left(\frac{v_y - l_r r}{v_x - (t_r/2)r}\right) \tag{17}$$

$$\alpha_{rr} = \arctan\left(\frac{v_y - l_r r}{v_x + (t_r/2)r}\right) \tag{18}$$

where δ_f is the front wheel steer angle.

The longitudinal wheel slip σ_{xi}(i=fl,fr,rl,rr) is defined as:

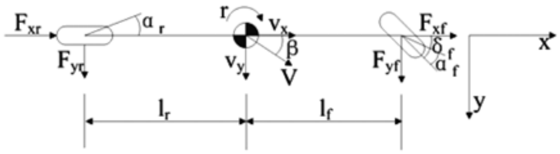

Figure 3. Single-track vehicle model.

$$\sigma_{xi} = \begin{cases} \dfrac{R\omega_i - v_x}{v_x} & during\ braking \\ \dfrac{R\omega_i - v_x}{R\omega_i} & during\ acceleration \end{cases} \tag{19}$$

with i =fl, fr, rl, rr.

3. PREVIOUS METHODS

3.1. Model-based Method

The estimation method based on the bicycle model (shown in Figure 3) is used for comparison in this paper. In Stephant *et al*. (2004), the yaw rate is employed to design the observer based on the linear bicycle model as follows:

$$\begin{cases} \dot{X} = AX + Bu \\ X = CX \\ \dot{\hat{X}} = A\hat{X} + Bu + G(Z - \hat{Z}) \\ \hat{Z} = C\hat{X} \end{cases}$$

with

$$X = (\beta_m\ \ r)^T, u = \delta_f,\ B = \left[\frac{C_f}{mv_x}\ \frac{C_f l_f}{I_{zz}}\right]^T,$$

$$Z = r,\ A = \begin{bmatrix} -\dfrac{C_f + C_r}{mv_x} & -1 - \dfrac{l_f C_f - l_r C_r}{mv_x^2} \\ -\dfrac{l_f C_f - l_r C_r}{I_{zz}} & -\dfrac{l_f^2 C_f + l_r^2 C_r}{I_{zz} v_x} \end{bmatrix} \tag{20}$$

β_m is the side slip angle output of single-track vehicle model. The linear observer proposed here is a Luenberger observer. Hence, the observer gain G can be easily selected by using the pole placement to guarantee the stability of the observer. The hatted quantity $\hat{\beta}_m$ is the model-based estimation of side slip angle. This model-based method normally achieves a sufficiently accurate estimation in the linear region of the tire characteristics, but the accuracy tends to degrade when the tire characteristics become nonlinear.

3.2. Kinematics-based Method

The kinematics-based method proposed in (Park *et al.*, 2001) is also known as the direct integration method. The kinematical relationship of the slip angle velocity, yaw rate, lateral acceleration, longitudinal velocity and road bank angle φ_r shown in equation (21) is used to estimate the vehicle slip angle.

$$a_y = (\dot{\beta}_k + r)v_x - g\sin\varphi_r \tag{21}$$

Then, direct integration is implemented to estimate the side slip angle.

$$\hat{\beta}_k = \int \dot{\hat{\beta}}_k dt = \int \left(\frac{a_y + g\varphi_r}{v_x} - r \right) dt \tag{22}$$

This method can achieve robustness against tire properties, road friction and vehicle parameters such as vehicle mass and moment of inertia. However, it is very sensitive to the inevitable sensor noises such as vehicle speed, lateral acceleration and yaw rate measurements, and road bank angle. The estimation can achieve significant deviation over time no matter how small the bias error is.

4. PROPOSED ESTIMATION METHOD

4.1. Side Force Calculation

The former mentioned single-track model shown in equation (20) is currently used to describe vehicle dynamic behavior. Hence, the side force can be estimated from the lateral acceleration and yaw rate with a simple vehicle parameter.

$$F_{yfs} = \frac{l_r m a_y + I_{zz}\dot{r} - M_z}{l} \tag{23}$$

$$F_{yys} = \frac{l_f m a_y - I_{zz}\dot{r} + M_z}{l} \tag{24}$$

M_z is the estimated yaw moment induced by braking control. The side force calculated from the sensor signal is robust against vehicle parameters, tire-road conditions and driving operations. However, it is very sensitive to sensor noise, which can cause large drift. To guarantee the performance of estimation in all operation regions, the combination of tire model and direct calculation from sensor is adopted. A linear adaptive tire model is also proposed here to give the side force estimation. The cornering stiffness $\hat{C}_f$ and $\hat{C}_r$ are derived from the adaptive identifier in real time. It is described in section 4.3.

$$F_{yfm} = \hat{C}_f \alpha_f \tag{25}$$

$$F_{yrm} = \hat{C}_r \alpha_r \tag{26}$$

The wheel slip angles can be derived from the yaw rate and the estimated vehicle slip angle from the proposed estimation method as:

$$\alpha_f = \hat{\beta} + \frac{l_f r}{v_x} - \delta_f \tag{27}$$

$$\alpha_r = \hat{\beta} - \frac{l_r r}{v_x} \tag{28}$$

The weighted sum of side forces can be calculated according to the nonlinear factor α, which is determined by the deviation of yaw rate from the reference value and vehicle lateral acceleration. A fuzzy logic is employed to identify the value in Section 4.2.

$$F_{yf} = \alpha F_{yfs} + (1-\alpha)F_{yfm} \tag{29}$$

$$F_{yr} = \alpha F_{yrs} + (1-\alpha)F_{yrm} \tag{30}$$

4.2. Nonlinear Factor Identifier

To judge whether the vehicle state is in the linear or nonlinear region, a nonlinear factor α is introduced to evaluate the degree of the nonlinear state. A fuzzy logic is implemented to calculate the nonlinear factor. The input variables are the deviation of the yaw rate Δr and lateral acceleration a_y. The proposed nonlinear factor is the output variable. Fuzzification is first implemented to convert the variable to linguistic variable. Table 1 shows the linguistic

Table 1. Linguistic terms.

NB	Negative big	PS	Positive small	M	Medium
NS	Negative small	PB	Positive big	L	Large
ZE	Zero	S	Small	VL	Very large

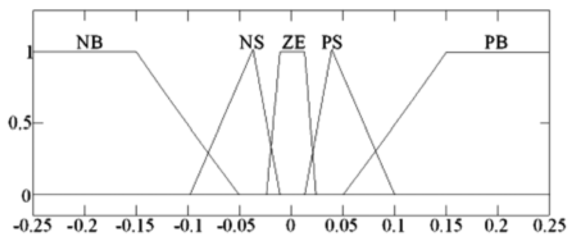

Figure 4. Membership function for Δr.

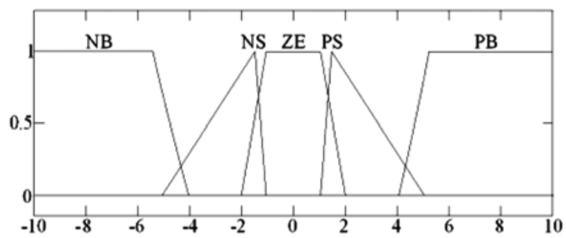

Figure 5. Membership function for a_y.

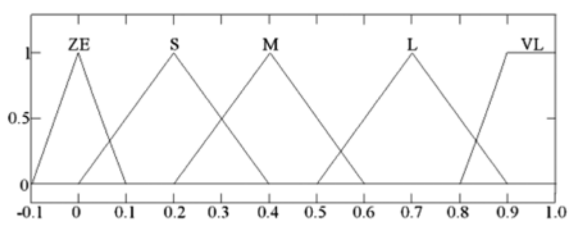

Figure 6. Membership function for α.

terms. The membership functions and ranges of values of the variables are shown in Figure 4, Figure 5 and Figure 6.

The yaw rate deviation Δr is defined as the deviation of the reference value and the measured yaw rate and converted to the slip angle dimension (Fukada, 1999).

$$\Delta r = \left(1+\left(\frac{v_x}{v_c}\right)\right)\frac{(r_{ref}-r)l}{v_x}\frac{|r|}{r} \tag{31}$$

The reference yaw rate can be calculated as:

$$r_{ref} = \frac{v_x}{l}\frac{\delta_f}{1+\left(\frac{v_x}{v_c}\right)^2} \tag{32}$$

where $v_c = \sqrt{\frac{l^2}{m\left(\frac{l_r}{C_f}-\frac{l_f}{C_r}\right)}}$ is the characteristic speed.

The reference value described above is calculated under high friction conditions. Hence, the yaw rate deviation can be used to detect the road condition. If the yaw rate is small, the friction coefficient of the road is high. If the yaw rate is large, the friction coefficient of the road is low.

The rules for the proposed fuzzy logic are shown in Table 2. These rules are introduced based on expert knowledge and the extensive simulations performed in this study. To guarantee the performance under different road conditions, the rules follow the next criteria:

Δr is small and a_y is small

In this case, the vehicle state is in the linear region. The nonlinear factor is considered to be small.

Δr is large and a_y is small

In this case, the vehicle is considered to be driving on low friction road. The nonlinear factor is mainly determined by the values of input variable Δr.

Δr is small and a_y is large

In this case, the vehicle is considered to be driving on high friction road. The nonlinear factor is mainly determined by the values of input variable a_y.

These criteria are the base of rules. The fuzzy logic uses the Mamdani Fuzzy Interface System. The weights of the rules are considered to be 1.

4.3. Cornering Stiffness Identifier

The tire cornering stiffness characterizing the tire-road interaction on the front and rear axles might be identified from experimental tests on the specific vehicle. However, it can be seriously influenced by tire- road friction condition and driving operation. The identified parameter derived from dry asphalt may give relatively incorrect reproduction of the vehicle behavior due to changes in the tire-road friction conditions. Moreover, the relation between the slip angle and lateral force becomes strongly nonlinear under severe operation. The linear model is unable to predict the vehicle dynamics. Hence, the cornering stiffness identifier is proposed to tune the cornering stiffness according to the degree of the vehicle nonlinear state in this paper. The nonlinear factor is introduced to calculate the cornering stiffness in real-time:

$$\hat{C}_f = \alpha C_f + (1-\alpha)C_{fs} \tag{33}$$

$$\hat{C}_r = \alpha C_r + (1-\alpha)C_{rs} \tag{34}$$

$$C_{fs} = \frac{F_{yfs}}{\alpha_f} \tag{35}$$

$$C_{rs} = \frac{F_{yrs}}{\alpha_r} \tag{36}$$

C_f and C_r are the values of the cornering stiffness identified from experimental tests under high friction conditions. C_{fs} and C_{rs} are the values of cornering stiffness obtained from the sensor signal in real-time.

Table 2. Rule base.

Yaw rate error	Lateral acceleration NB	NS	ZE	PS	PB
NB	VL	L	L	L	VL
NS	L	L	M	L	L
ZE	M	S	S	S	M
PS	L	L	M	L	L
PB	VL	L	L	L	VL

4.4. Extended Kalman Filter Design

After a preliminary estimation of the vehicle lateral force is calculated, it is fed into an observer, which provides the final estimate of the vehicle side slip angle. The observer is constructed from a simplified single-track model with a linear adaptive tire-force model. The adaptive cornering stiffness identifier is introduced here to guarantee good estimation results under severe maneuvers and different road conditions. In addition, the effect of the tire force lag on the vehicle dynamics is also taken into account (He *et al.*, 2006). The dynamics of the observer can be described by the following equations:

$$\begin{cases} \dot{\beta} = \dfrac{F_{yf}\cos(\delta_f-\beta)+F_{yr}\cos(\beta)}{mv_x} - r \\ \dot{F}_{yf} = \dfrac{(-F_{yf}+F_{yfss})}{\tau_{yf}} \\ \dot{F}_{yr} = \dfrac{(-F_{yr}+F_{yrss})}{\tau_{yr}} \end{cases} \tag{37}$$

with $\tau_{yf} = \tau_{yr} = RL_y/v_x$ $F_{yfss} = \hat{C}_f\alpha_f$ $F_{yrss} = \hat{C}_r\alpha_r$

RL_y is the lateral tire relaxation length. τ_{yf} and τ_{yr} are the time constant of front and rear axle, respectively. F_{yfss} and F_{yrss} are the steady state values of the vehicle lateral forces. In this paper, the linear adaptive model described in section 4.1 is adopted to calculate the steady state value.

For the Kalman filter design, the following discrete state-space representation is adopted to determine the proper filter gain:

$$\begin{cases} x_{k+1} = f(x_k) + g(x_k, u_k) + w_k \\ y_k = h(x_k, u_k) + v_k \end{cases} \tag{38}$$

with

$$x_k = [\beta, F_{yf}, F_{yr}]^T, u_k = [\delta_f, r, v_x]^T, y_k = [F_{yf}, F_{yr}, a_y]^T$$

where the w_k is the process noise vector and v_k is the measurement noise vector. This noise is assumed to be Gaussian, white and centered with known covariance.

The extended Kalman filter design can be divided into three steps. The first step is to linearize the evolution equation around the estimated state and input. The Jacobian resulting from the Taylor series expansions are calculated as:

$$F = \frac{\partial f(x_k)}{\partial x_k}(\hat{x}_{k-1}, u_{k-1}, 0) \tag{39}$$

$$F = \frac{\partial h(x_k)}{\partial x_k}(\hat{x}_{k-1}^-, u_{k-1}, 0) \tag{40}$$

$$W = \frac{\partial f(x_k)}{\partial w_k}(\hat{x}_{k-1}, u_{k-1}, 0) \tag{41}$$

$$V = \frac{\partial h(x_k)}{\partial x_k}(\hat{x}_{k-1}^-, u_{k-1}, 0) \tag{42}$$

where F is the system model Jacobian, H is the output model Jacobian, W is the process noise Jacobian, and V is the measurement noise Jacobian.

The second step is to predict the next state from the previous state and measurement:

$$\hat{x}_k^- = f(\hat{x}_{k-1}, u_{k-1}, 0) \tag{43}$$

$$P_k^- = FP_{k-1}F^T + WQ_{k-1}W^T \tag{44}$$

The third step is to calculate the Kalman gain matrix, which is used to correct the state vector in line with measurement errors:

$$K_k = P_k^- H^T (HP_k^- H^T + VR_k V^T)^{-1} \tag{45}$$

$$\hat{x}_k = \hat{x}_k^- + K_k(y_k - h(\hat{x}_k^-, 0)) \tag{46}$$

$$P_k = (I - K_k H) P_k^- \tag{47}$$

The parameters are assumed to vary independently. The noise and system model are kept constant. The covariance matrixes are chosen as:

$$Q = diag[10^{-13}, 100, 100], \quad R = diag[0.1, 0.1, 0.1]$$

where Q and R are the noise covariance matrixes for w_k and v_k, respectively.

Table 3. Vehicle parameters.

m	Vehicle mass: 2325 kg
m_s	Sprung mass of the vehicle: 2090 kg
m_{uf}, m_{ur}	Front, rear unsprung mass: 138 kg, 97 kg
g	Gravitational acceleration: 9.81 m/s^2
I_{xx}	Roll moment of inertia: 750 kgm^2
I_{zz}	Yaw moment of inertia: 3500 kgm^2
I_{xz}	Yaw/roll product of inertia: 25 kgm^2
I_ω	Wheel spin moment of inertia: 2.1 kgm^2
t_f, t_r	Front, rear wheel track: 1.7 m, 1.7 m
l	Wheel base: 2.8 m
l_f, l_r	CG to front, rear axle distance: 1.05 m, 1.75 m
l_{fs}, l_{rs}	Sprung CG to front, rear axle distance: 1.07 m, 1.73 m
h_{cg}	Height of vehicle CG: 0.925 m
h_s	Sprung mass CG to roll axis distance: 0.6 m
h_{uf}, h_{ur}	Height of front, rear unsprung mass CG: 0.535 m, 0.535 m
R_ω	Tire rolling radius: 0.35 m
$K_{\varphi f}$, $K_{\varphi r}$	Front, rear suspension roll stiffness: 48000 Nm/rad, 38000 Nm/rad
$C_{\varphi f}$, $C_{\varphi r}$	Front, rear suspension roll damping: 2800 Nms/rad, 2600 Nms/rad
C_σ, C_σ	Tire longitudinal, lateral stiffness: 60000 N/unit slip, 40000 N/rad
C_f, C_r	Cornering stiffness of front, rear axle: 80000 N/rad, 80000 N/rad

5. SIMULATION RESULTS

A simulation was conducted to evaluate the performance of the proposed estimation method. Simulation results were obtained using the 8 DOF vehicle model in MATLAB and SIMULINK. The vehicle parameters are shown in Table 3. To clarify the performance of the proposed estimation method, the comparisons among the results of proposed method, the kinematics-based method and the model-based method are shown.

The effectiveness of proposed method is shown by considering three different road conditions. Figure 7 shows the front wheel steering angle of the maneuver implemented in the simulation test. The normalized error for an estimation z shown in equation (48) is introduced to present the estimation results.

$$\varepsilon_z = 100\frac{(\|z - z_{measurement}\|)}{\max(z_{measurement})} \tag{48}$$

To consider the effect of sensor noises, constant noise was introduced to contaminate the sensor signals. The

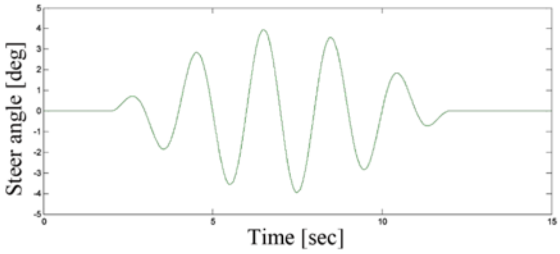

Figure 7. Steering input.

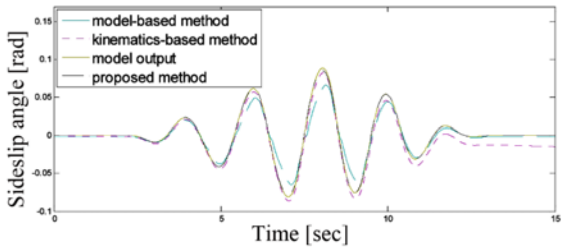

Figure 8. Slip angle estimation results on high friction road.

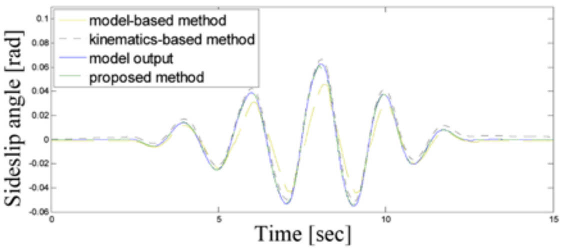

Figure 9. Slip angle estimation results on medium friction road.

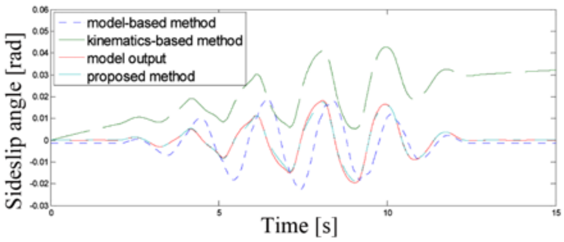

Figure 10. Slip angle estimation results on low friction road.

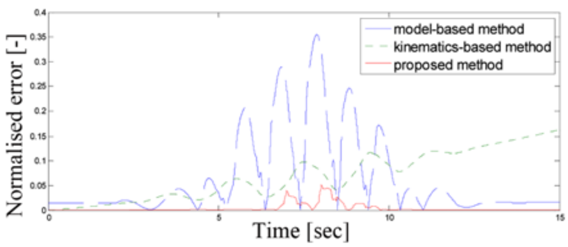

Figure 11. Normalized error on high friction road.

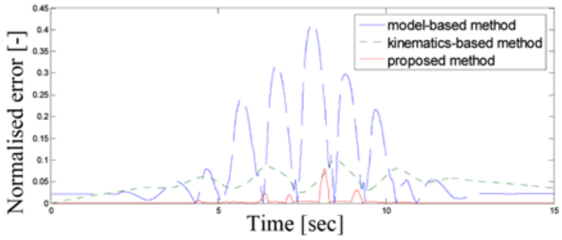

Figure 12. Normalized error on medium friction road.

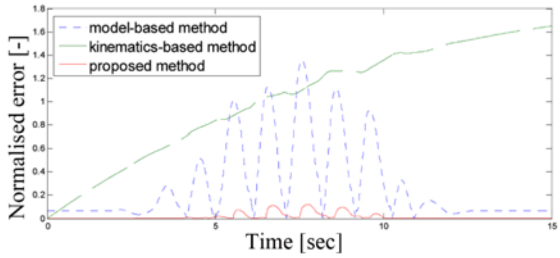

Figure 13. Normalized error on low friction road.

noise levels for lateral acceleration, yaw rate were set to be 0.1 m/s^2, 0.005 rad/s, respectively.

Figure 8 shows the simulation results of high friction road conditions (μ=0.8). The vehicle runs at the initial velocity of 22.22 m/s. The estimated slip angle using the kinematics-based method generates a drift due to the effect of integrating bias error. The estimation based on the model-based method follows the trend of measured value quite well in the linear region. However, some large errors still exist due to the modeling mismatch in nonlinear region. The proposed method combines the advantages of the previous two methods. It can reduce the effects of sensor noise and modeling mismatch. The estimation is accurate and smooth with a minimal phase lag. Figure 11 shows the normalized errors of the three estimation methods. The error of the kinematics-based method becomes larger during the estimation. It can be considered as the effect of sensor noise. The error of model-based method is large when the steer angle is large. Hence, the model-based method can give good estimation within the linear region. The error of proposed method is relatively small compared with the former two methods. According to the statistical results shown in table 4, the proposed method has the smallest maximum (5.1%) and mean values (0.388%); the maximum and mean values of the kinematics-based method are 16.3% and 7%, respectively; and the maximum and mean values of model-based method are 35.5% and 6.4%, respectively.

The estimation results on medium friction road are shown in Figure 9. The friction coefficient of the medium road was set to be 0.5 in this paper. The initial speed of vehicle was 16.67 m/s. The kinematics-based method can follow the trend of the measured value. However, relatively

Table 4. Normalized estimation errors.

Road friction	Model-based		Kinematics-based		proposed	
	Maximum	Mean	Maximum	Mean	Maximum	Mean
High	0.355	0.064	0.163	0.070	0.051	3.88e-3
Medium	0.417	0.078	0.099	0.047	0.08	3.07e-3
Low	1.352	0.280	1.649	1.024	0.122	0.015

large errors still exist due to the effect of sensor noise. The model-based method shows the largest estimation error, which is much worse than that on the high friction road, mainly because of the modeling mismatch such as inaccurate values of the cornering stiffness. The estimation results of the proposed method can accurately track the measured value. Figure 12 shows the normalized error of each estimation method in medium friction conditions. According to the statistical results shown in table 4, the proposed method has the smallest maximum (8%) and mean values (0.307%); the maximum and mean values of kinematics-based method are 9.9% and 4.7%, respectively; and the maximum and mean values of model-based method are 41.7% and 7.8%, respectively.

The low fiction coefficient was set to be 0.2 in this paper. The vehicle initial velocity was 11.11 m/s. Figure 10 shows the simulation results. Similar results can be obtained compared with the high friction and low friction conditions. The kinematics-based method cannot overcome the effect of sensor noise, and the model-based method is influenced by model mismatch. However, the proposed method shows great robustness against sensor noise and model mismatch. Figure 13 shows the normalized error of estimation results on a low fiction road. According to the statistical results shown in table 4, the proposed method has the smallest maximum (12.2%) and mean values (1.5%); the maximum values of the kinematics-based method and model-based method are 164.9% and 135.2%, respectively; and the mean values of the kinematics-based method and model-based method are 102.4% and 28%, respectively. In all, the kinematics-based method is greatly influenced by sensor noise. The model-based method can generate satisfactory estimation in linear region. However, the estimation is inaccurate in the nonlinear region. The proposed method can provide accurate estimation, which is robust against sensor noise and modeling error, and it can guarantee estimation accuracy under different road friction conditions.

6. CONCLUSION

A method for vehicle side slip angle estimation is proposed in this paper. The side force is obtained as a weighted mean of two different predictions: the first one derived from the sensor signal based on a kinematics-based method and the second one calculated from a linear adaptive tire model. Then, the predicted side forces are fed to the extended Kalman filter based on a vehicle single model associated with a linear adaptive tire model to give the ultimate estimation of the side slip angle. The tire cornering stiffness identifier is defined to take into account changes in the tire-road interaction. A nonlinear factor is proposed to classify the degree of vehicle nonlinear states. A fuzzy logic is implemented to calculate the nonlinear factor.

A simulation was conducted to evaluate the performance of the proposed method under severe maneuvers on different road conditions. The simulation results were compared with the kinematics-based method and model-based method. The proposed method achieved observable improvement with respect to the previous method. It can give satisfactory results in different road friction conditions.

Future developments of this research will focus on the implementation of the proposed estimation method on vehicles for experimental tests in real-time.

ACKNOWLEDGEMENT−This work was supported by National Natural Science Foudation (No.50975047); National Natural Science Foudation (No.50575041); Research Foundation of SAIC motor (No.20070101); Nanjing Science and Technology Program (No.2703030).

REFERENCES

Bevly, D. M., Ryh, J. and Gerdes, J. C. (2006). Integrating INS Sensors with GPS measurements for continuous estimation of vehicle sideslip, roll, and tire cornering stiffness. *IEEE Trans. Intelligent Transportation Systems* **7**, **4**, 483−493.

Cheli, F., Sabbioni, E., Pesce, M. and Melzi, S. (2007). A methodology for vehicle sideslip angle identification: Comparison with experimental data. *Vehicle System Dynamics* **45**, **6**, 549−563.

Chen, B. C. and Hsieh, F. C. (2008). Sideslip angle estimation using extended Kalman filter. *Vehicle System Dynamics*, **46**, Supplement, 353−364.

Daily, R. and Bevly, D. M. (2004). The use of GPS for vehicle stability control systems. *IEEE Trans. Industrial Electronics* **51**, **2**, 270−277.

Dugoff, H., Fancher, P. S. and Segel, L. (1970). An analysis of tire traction properties and their influence on vehicle dynamic performance. *SAE Paper No.* 700337.

Fukada, Y. (1999). Slip-angle estimation for vehicle stability control. *Vehicle System Dynamics*, **32**, 375−388.

Hac, A. and Simpson, M. D. (2000). Estimation of vehicle sideslip angle and yawrate. *SAE Paper No.* 2000-10-0696.

He, J., Crolla, D. A., Levesley, M. C. and Manning, W. J. (2006). Coordinaation of active steering, driveline, and braking for integrated vehicle dynamics control. *Proc. IMechE Part D: J. Automobile Engineering*, **220**, 1401−1421.

Hiraoka, T., Kumamoto, H. and Nishihara, O. (2004). Sideslip angle estimation and active front steering system based on lateral acceleration data at centers of percussion with respect to front/rear wheels. *JSAE Review*, **25**, 37–42.

Jo, J. S., You, S. H., Joeng, J. Y., Lee, K. Y. and Yi, K. (2008). Vehicle stability control system for enhancing steerability, lateral stability, and roll stability. *Int. J. Automotive Technlogy* **9**, **5**, 571–576.

Keinke, U. and Daiβ, A. (1997). Observation of lateral vehicle dynamics. *Control Engineering Practice* **5**, **8**, 1145–1150.

Mammar, S. and Koenig, D. (2002). Vehicle handling improvement by active steering. *Vehicle System Dynamics*, **38**, 211–242.

Masato, A., Yoshio, K., Kazuasa, S., Yasuji, S. and Yoshimi, F. (2001). Side-slip control to stabilize vehicle lateral motion by direct yaw moment. *JSAE Review*, **22**, 413–419.

Nishio, A., Tozu, K., Yamaguchi, H., Asano, K. and Amano, Y. (2001). Development of vehicle stability control system based on vehicle side slip angle estimation. *SAE Paper No.* 2001-01-0137.

Park, K., Heo, S. J. and Baek, I. (2001). Controller design for improving lateral vehicle dynamic stability. *JSAE Review*, **22**, 481–486.

Piyabongkarn, D., Rajamani, R., Grogg, J. A. and Lew, J. Y. (2006). Development and experimental evaluation of a slip angle estimator for vehicle stability control. *Proc. PACC,* 366–5371.

Stephant, J., Charara, A. and Meizel, D. (2004). Virtual sensor: Application to vehicle sideslip angle and transversal forces. *IEEE Trans. Industrial Electronics* **51**, **2**, 278–289.

Van Zanten, A. T. (2000). Bosch ESP systems: 5years of experience. *SAE Paper No.* 2000-01-1633.

Van Zanten, T., Erhardt, R. and Pfaff, G. (1996). Control aspects of bosch-VDC. *Proc. AVEC,* 573–607.